JOURNAL OF SOLID STATE CHEMISTRY 58, 325–334 (1985)

A Study of the Mixed $Na_{1-x}Li_x$ Zeolite A System by Powder X-Ray Diffraction

J. M. NEWSAM, R. H. JARMAN, AND A. J. JACOBSON

Exxon Research and Engineering Company, Clinton Township, Annandale, New Jersey 08801

Received June 20, 1984; in revised form December 18, 1984

A simple analysis of the ratios of selected X-ray powder diffraction intensities from anhydrous sodium-lithium zeolite A samples, $Na_{12-x}Li_xSi_{12}Al_{12}O_{48}$, shows that Li replaces Na in site I for $0 \leq x \leq 8$. This result is discussed in relation to previously reported ^{29}Si NMR data and a model is presented for the cation ordering scheme in the anhydrous mixed material with $x = 4$. Changes in the X-ray pattern with external water vapor pressure are also described.

Introduction

Three crystallographically distinct cation sites have been determined in anhydrous sodium zeolite A from single crystal X-ray diffraction data (*1, 2*). Eight of the 12 cations per 12.3-Å subcell are contained in the six-ring, site I (Fig. 1 and Ref. (*3*)), which has full occupancy. The sites of type II house one Na^+ ion per eight-ring window, or a total of three in each subcell, and the remaining Na^+ ion is found at a site of type III. Although the structure of the hydrated material is less precisely known, the cation sites and populations appear to be little changed except that the position of the single Na^+ ion which occupies site III in the anhydrous material was not determined (*4*).[1]

[1] The coordinates of site II are not explicitly given in Ref. (*4*), although "site IV" (0.041, 0.210, 0.235) is about 1.1 Å from cation site II (0, 0.211, 0.217) of Ref. (*2*). The disorder associated with species other than the framework and Na(1) made it impossible to assign electron density unambiguously to other cations or sorbed water.

In the mixed system $Na_{1-x}Li_x$–A, distinct site preferences for the two cations in both hydrated and anhydrous forms are reflected in the thermodynamics of ion exchange and the zeolite's sorption properties. The heats of partial exchange (ΔH_x^0) determined calorimetrically at 25°C show a discontinuity at $x \approx 0.35$. For $x < 0.35$, ΔH_x^0 is constant and near zero. For $x > 0.35$, ΔH_x^0 rises linearly with x (*6*). Reflecting these differences, the ion-exchange isotherms in the range 5–65°C are temperature independent for $x < 0.35$, but for $x > 0.35$, they show significant temperature dependence. The inflection which is observed at the transition point between the two regimes, $x \approx 0.35$ becomes more pronounced as the exchange temperature decreases (*7*). In interpreting these data on fully hydrated materials, Barrer *et al.* (*6*) assigned the range up to $x = 0.33$ to selective replacement of the Na^+ ions more closely associated with the zeolitic water (namely sites II and III), exchange beyond $x = 0.33$ corresponding to replacement of the Na^+ ions in site I.

In anhydrous $Na_{1-x}Li_x$–A, *n*-hexane

0022-4596/85 $3.00

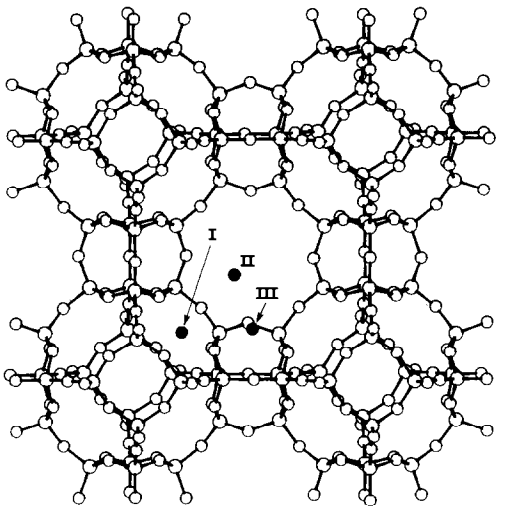

FIG. 1. A representation of one half of the 12.3-Å subcell of sodium zeolite A drawn with the aid of the CHEMGRAF package (*5*). The filled circles indicate the locations of sodium ions at site I (center of the six-ring window), site II (statistically offset from the center of the eight-ring window), and site III (in the large cage opposite the four-ring window). Only one of the several symmetry equivalent positions for each cation site is shown. Of the open circles, the smaller represent oxygen and the larger Si or Al atoms.

sorption studies apparently indicate different changes in site preference with increasing lithium content (*8*). The capacity of the zeolite for *n*-hexane remains low until $x > 0.7$ beyond which it increases rapidly with x up to complete exchange of Na^+ by Li^+. This behavior is consistent with Li^+ replacing Na^+ in site I selectively, the residual Na^+ ions in site II effectively blocking pore windows to *n*-hexane absorption, until they too are exchanged. This picture is largely confirmed by powder neutron and X-ray diffraction analyses of samples with $x = 0.80$. Although of modest precision, these indicate that the bulk of the lithium ions have replaced most of the sodium ions at site I (*9*).

Further information on the system is provided by solid-state nuclear magnetic resonance (NMR). High-resolution ^{29}Si NMR studies of several zeolites show that replacement of Na^+ by Li^+ typically results in a shielding by 4–5 ppm of the ^{29}Si resonances (Table I). A detailed study of the $Na_{1-x}Li_x$–A system using both ^{29}Si and ^7Li NMR spectroscopy (*10*) again indicated cation ordering which depends on the degree of hydration. The data on near anhydrous materials which show a distinct discontinuity at $x = 0.33$ were interpreted as resulting from replacement of Na^+ at site I by Li^+ up to this level. These first four lithium ions per subcell effect the major proportion of the change in the ^{29}Si chemical shift. Subsequent substitution by more lithium ions at site I has a smaller effect, as does Li^+ exchange at sites II and III. The ^{29}Si NMR chemical shift variation for the hydrated materials was then interpreted by allowing partial exchange of Na^+ and Li^+ between sites I and II (*10*).

The spectroscopic and exchange or sorption techniques referred to above do not directly determine the cation site populations, and in order to understand the structural changes that underly these observations, we undertook a series of diffraction experiments. Specifically, we have used reflection intensity ratios from powder X-ray diffraction data to monitor the sites of cation exchange in $Na_{1-x}Li_x$–A. This approach, although it does not provide complete structural information, proves ade-

TABLE I

^{29}Si NMR CHEMICAL SHIFTS AND MEAN Si–O–*T* ANGLES FOR SOME Na- AND Li-ZEOLITES

Material	Si(4Al) ppm vs TMS	Ref.	Si–O–*T* (°)	Ref.
Na-A	−89	*25, 26*	149	*2*
Li-A	−85	*10*	141	*21*
Na-*X*	−85	*25*	139	*23*
Li-*X*	−80	*27*	—	—
Na-Cancrinite	−87	*26*	142	*22*
Li, Na-Cancrinite	−82	*26*	—	—
Li-A(BW)	−80	*26*	135	*24*

quate for following changes in the cation site populations as a function of composition.

Experimental

The parent samples of sodium zeolite A were either commercial Linde 4A material or as crystallized from a standard gel formulation (*11*). Chemical analysis, X-ray powder diffraction, and ^{29}Si NMR data indicated that both materials were high-quality zeolite A. Ion exchange was achieved as in Ref. (*11*). Chemical compositions were determined by inductively coupled plasma emission spectroscopy.

Powder X-ray diffraction measurements were made under controlled humidity using a Philips vertical diffractometer and Cu$K\alpha$ radiation. Samples were dehydrated by heating in air or under vacuum at 400°C for several hours and then loaded under dry helium into a hermetically sealed stainless-steel sample holder with a Be window. In addition to the anhydrous scans on each sample, some measurements were made with the cell attached *in situ* to a gas-flow line in which dry nitrogen, and nitrogen saturated with water at ambient temperature, were mixed in the desired proportion. The partial pressure of water in the exit line from the cell was monitored with a General Eastern 1200 AP dew-point hygrometer. Powdered quartz or α-Al_2O_3 was used as an internal standard and lattice parameters were obtained from reflections in the range $10° < 2\theta < 40°$ using least squares or simple averaging. Reflection intensities were determined by triangulation or by cutting and weighing copies of the scans on viewgraph plastic sheets.

Reflection Intensity Ratios

A rigorous analysis of the changes in structure associated with a particular cation composition requires a complete structure determination using single crystal or, perhaps, Rietveld powder profile analysis techniques (*12, 13*). In both these techniques, a definitive result requires that all features of the measured diffraction pattern be well fitted by that calculated. However, the nature of the structure factor expression is such that not all atomic species contribute equally to all the diffracted intensities. This then allows the possibility of extracting from the observed diffraction pattern those features which are sensitive only to a particular atomic parameter of interest. As some reflections will be enhanced and others diminished by a change in a particular atomic parameter, the use of selected reflection intensity ratios provides further sensitivity. Indeed, there are already several examples of the use of powder diffraction intensity ratios in determining quantitative structural information (*14*). In zeolite chemistry this approach has previously been applied to locate the positions of rare earth cations in faujasites (*15*). In the present case, we have extended this approach to monitoring the sites of lithium exchange in sodium zeolite A across the Na–Li composition field.

The contribution, $C(hkl)$, of a particular atomic species to the structure factor $F(hkl)$ can be estimated in two ways:

$$C_1(hkl) = 1 - \frac{|F_{\text{diff}}(hkl)|}{|F(hkl)|}$$

$$C_2(hkl) = \frac{|F_{\text{atom}}(hkl)|}{|F(hkl)|},$$

where $F_{\text{diff}}(hkl)$ is the structure factor computed excluding the selected atom, and $F_{\text{atom}}(hkl)$ is the structure factor computed including only that atom. Both calculations are inexact since the phasing of the atomic contribution with that of the remainder of the cell is not accounted for. However, they indicate which reflections merit closer scrutiny. The cation contributions to each reflection can then be monitored more exactly by calculating intensities based on the

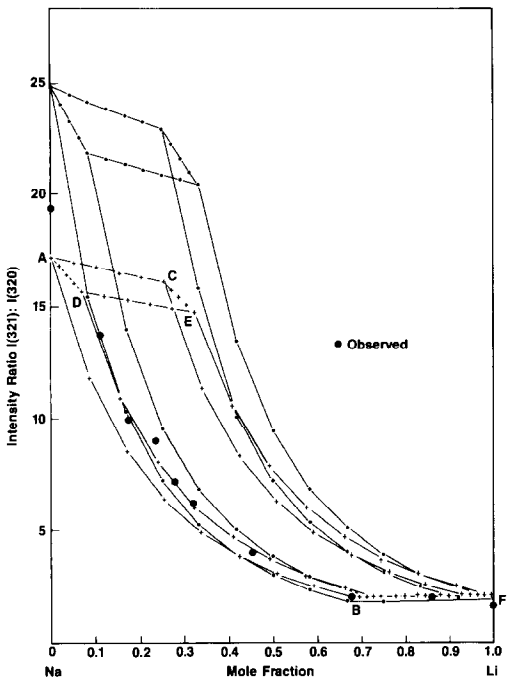

FIG. 2. Calculated ratios of the intensities of the 321 and 320 reflections plotted against the extent of lithium exchange. Each curve indicates the values calculated for lithium substitution at one of the three cation sites, based on the atomic coordinates given in Refs. *2* (+) or *9* (·), respectively. The range of composition that a given curve spans indicates which site is being exchanged (I ≫ II > III). Thus AB indicates Li substitution in site I, AC in II, AD in III, CE in III following complete exchange of II, etc. The observed ratios for 10 compositions are also plotted. The estimated experimental errors on the observed ratios vary from ±5 at $x = 0$, through ±1 at $x = 0.3$ to ±0.1 at $x = 1.0$.

entire structure, while allowing each cation site occupancy to vary separately in discrete increments.

The above calculations were computed for the $Na_{1-x}Li_x$–A system using simple modifications of existing structure factor routines. Taking both the atomic parameter data of Pluth and Smith (24.555-Å supercell, $Fm\bar{3}c$) (*2*) and those of Jirak *et al.* (1196-Å subcell, $Pm3m$) (*9*) as basis models, intensities were calculated for a set of reflections with $0° < 2\theta < 40°$ as sodium was replaced incrementally by lithium in each cation site, permuting all combinations. In this way, the complete composition field, $0 < x < 1$, was covered for both models. In both sets of calculations the lithium coordinates were assumed to be identical to those of sodium and vice versa (The X-ray scattering power of Li^+ is small so that slight changes in the lithium location do not grossly affect the calculated intensities). Comparison of the Pluth and Smith (*2*) and Jirak (*9*) structures indicates that the framework is distorted in accommodating the smaller lithium cations. Calculation using the two sets of atomic coordinates enabled us to select those reflection intensity ratios that are relatively insensitive to this framework distortion. Atomic scattering factors for Si^{2+}, Al^+, O^-, O (for H_2O), Na^+ and Li^+ were taken from International Tables (*16*).

Results and Discussion

Anhydrous Materials

The calculated behavior for one intensity ratio, $I(321):I(320)$, for all combinations of sequential exchange of the three cation sites together with observed data points is shown in Fig. 2. Observed and calculated data for three selected intensity ratios are given in Table II. The data demonstrate that several intensity ratios that are insensitive to small changes in framework geometry vary markedly depending on which cation sites are exchanged. Such ratios therefore provide a reliable indication of the sites of cation substitution. For other ratios, such as $I(311):I(420)$, values calculated on the basis of the Pluth and Smith coordinates are substantially different from those derived with the Jirak model. Although such ratios could thus be used to monitor framework distortion, they cannot provide reliable information about cation site populations. In the present case, it is the availability of structural data at two

TABLE II

CALCULATED AND OBSERVED REFLECTION INTENSITY RATIOS[d] FOR $Na_{12-x}Li_x$–A MATERIALS

			Na_8		Na_4		
Model[a]	Ratio	Na_{12}	I[b]	III, II[c]	I[b]	III, II, I[c]	Na_0
PS	321/320	17.2	5.00	14.8	2.06	4.73	2.09
J		24.9	5.29	20.4	1.88	5.15	1.98
Observed		19.3	4.46		2.09		1.64
PS	311/321	1.52	1.84	1.18	2.27	1.42	1.74
J		1.22	1.74	0.92	2.40	1.23	1.68
Observed		1.74	1.72		2.35		2.47
PS	(322 + 410)/320	20.7	6.32	15.2	2.82	5.01	2.34
J		26.6	7.11	21.2	2.80	5.62	2.31
Observed		25.7	5.77		2.91		2.80

[a] PS and J indicate atomic coordinates taken from Pluth and Smith (*2*) and Jirak *et al.* (*9*), respectively. The indices are those based on the a_0 = 12 Å subcell. Although the strict alternation of silicon and aluminum that occurs in the zeolite A structure gives rise to a $2a_0 \times 2a_0 \times 2a_0$ supercell (*4*), the superlattice reflections are weak and use of the subcell does not significantly affect the results.

[b] Calculated for substitution of Li for Na only at site I.

[c] Calculated for substitution of Li for Na at site III, then site II (then, if necessary, site I).

[d] The estimated errors in the intensity ratios depend on the ratios themselves and hence vary across the composition field. The estimated errors are largest when the denominator in the ratio is the intensity of a weak peak. For the $I(321):I(320)$ ratios listed here and shown in Fig. 2, for example, the estimated errors vary from ±5 at $x = 0.0$, through ±1 at $x = 0.3$, to ±0.1 at $x = 1.0$.

compositions that enables recognition of those ratios which do probe cation occupations throughout the intervening composition range.

For the parent sodium form, both observed intensities and intensity ratios agree well with those calculated from the Pluth and Smith model (see Table III below). The data for the mixed materials given in Table II and shown in Fig. 2 indicate that lithium substitution in the anhydrous materials occurs initially at sites III and I. The estimated experimental uncertainty on the $I(321):I(320)$ ratio is greatest at lower lithium loadings where the intensity of the 320 reflection is smallest (see footnote to Table II). Further, the diffraction data is relatively insensitive to changes in the site III population as the total occupancy of each of the type III sites is small. Thus, although the data shown in Fig. 2 apparently indicate initial substitution at site III followed, at slightly higher lithium loadings, by exchange of the site I sodium ions, we cannot conclusively exclude, for example, the possibility of initial simultaneous replacement of the sodium cations at a combination of sites I and III. Because of its low occupancy, however, the exact position in the composition field at which site III exchange occurs does not affect our conclusions and in the subsequent discussion we focus on the partitioning between sites I and II, to which the diffraction data provides good sensitivity (Table II and Fig. 2). The data demonstrate that the site I/III occupancy increases continuously with increasing x within the composition range $0 < x < 0.67$, and that only when site I/III has been completely exchanged is site II affected. In the

TABLE III

POWDER X-RAY DIFFRACTION INTENSITIES[j] FOR Na_{12}–A AND Na_8Li_4–A AT VARIOUS STATES OF HYDRATION

	$Na_{12}Li_0$–A					Na_8Li_4–A					
	Anhydrous		Ambient		20 mm Hg	Anhydrous		Ambient			20.6 mm Hg
hkl	Obsd	Calcd[a]	Obsd	Calcd[b]	Obsd	Obsd	Calcd[c]	Obsd	Calcd I[d]	Calcd II[e]	Obsd
221 300	67	70	62	75	58	65	67	80	76	75	50
310	0	1	4	3	3	0	2	11	4	3	7
311	100	100	100	100	97	100	100	100	100	100	82
222	4	3	3	2	0	0	1	0	0	1	0
320	3	4	24	22	25	13	11	40	33	27	42
321	58	66	80	92	78	58	54	72	84	89	80
410 322	77	79	97	88	100	75	69	87	80	84	100
411 330	10	12	17	16	20	8	16	11	19	17	12
420	9	10	21	20	21	6	8	13	14	17	17
421	6	7	8	7	8	14	8	10	8	7	12
332	57	60	63	60	68	62	47	63	52	56	87
R_I[f]	5.9		9.2		13.6	12.0		12.1[g]		13.8[h]	26.4[i]

[a] Atomic coordinates taken from Pluth and Smith (*2*).
[b] Atomic coordinates taken from Gramlich and Meier (*4*).
[c] As footnote *a*, with equal populations of Na^+ and Li^+ at site I.
[d] As footnote *b*, with equal populations of Na^+ and Li^+ at site I.
[e] As footnote *b*, with site-I composition Na_3Li.
[f] Residual based on listed intensities, $R_I = \Sigma|I_{obs} - I_{cal}|\Sigma I_{obs}$.
[g] I_{obs} at ambient humidity, I_{cal} as footnote *d*.
[h] I_{obs} at ambient humidity, I_{cal} as footnote *e*.
[i] I_{obs} at P_{H_2O} = 20.6 mm Hg, I_{cal} as footnote *d*.
[j] The intensities are given rounded to the nearest integer. The ratios given in Table II were computed using nonrounded values for the intensities.

pure lithium form, Na_0Li_{12}–A, the calculated ratios are not in such good agreement with those observed, presumably indicating changes in structure that are not described by either the Pluth and Smith or Jirak models.

The X-ray diffraction analysis shows that the lithium occupancy of site I increases continuously up to $x = 0.67$. The variation of the cubic unit cell edge with composition (Fig. 4), however, is linear up to $x \approx 0.33$ but beyond this point is more gradual and nonlinear. The nmr data also shows a discontinuity at $x = 0.33$ in the plot of ^{29}Si chemical shift against composition (*10*). Smith and Blackwell (*17*) recently demonstrated a linear relationship between the magnitude of the ^{29}Si chemical shift and the mean secant of the Si–O–Si angles in a range of silicas. A collation of data on chemical shifts for silicon surrounded by four aluminum atoms [Si(4Al)] and Si–O–Al angles derived from structural data for several Na- and Li-zeolites is included in Table I. The structural dependence of the chemical shift of the Si(4Al) environment is at least qualitatively similar to that of the Si(4Si) environment in other zeolites (*18*, *19*) and silica polymorphs (*17*). The change in the magnitude of the chemical shift with

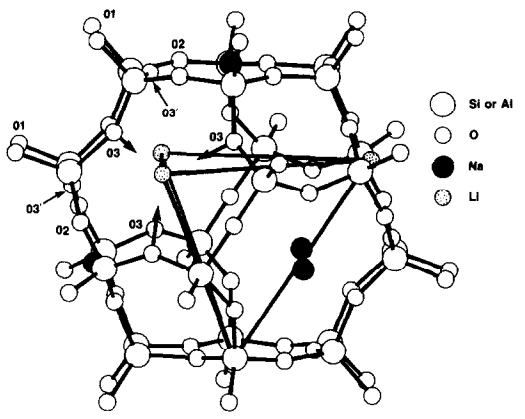

FIG. 3. A single sodalite cage containing 4 Na^+ and 4 Li^+ at the six-ring windows (site I), drawn with the aid of the CHEMGRAF package (*5*). Optimal coordination of the smaller Li^+ cations requires an adjustment of the O3 coordinates (indicated by arrows). A similar displacement cannot simultaneously occur for both such oxygens, O3 and O3′, in any given tetrahedron. This then gives rise to a proposed interpenetrating tetrahedral arrangement of the cations as shown (the heavy black lines are shown connecting the four lithium ions).

lithium substitution thus apparently reflects a change in the mean Si–O–Al angle, a consequence of cation exchange. It does not indicate how the individual Si–O–Al angles (of which there are three in zeolite A) are changing.

In sodium zeolite A (*2*), the *T*–O–*T* (*T* = tetrahedral species, Si or Al) angles are 142° (about O1), 165° (O2), and 145° (O3). There are twice as many linkages through O3 as there are through O1 or O2, so that the mean *T*–O–*T* angle is 149° (Table I). In $Na_{0.2}Li_{0.8}$–A (*9*), these angles are 176° (O1), 130° (O2) and 134° (O3). The site-I cation is coordinated by three O3's (Fig. 3). Substitution of sodium by the smaller lithium cations results in a shift of O3 towards the lithium, decreasing the *T*–O3–*T* angle. As the TO_4 tetrahedra remain essentially regular, there are only a limited number of ways in which this distortion can be accommodated. A complete description of these modes would require a detailed analysis similar to those that have been reported for structures comprised of corner-linked *octahedra* (*20*). A qualitative picture is, however, accessible through manipulation of three-dimensional models.

Inspection of Fig. 3 indicates that the distortion required to decrease the O3–Li distance and, correspondingly, the *T*–O3–*T* angle is facile only for two (opposite) oxygen atoms O3 in any four-ring window. The adjustment of the TO_4 tetrahedron (crystallographically $T[O1{\cdot}O2{\cdot}O3_2]$) is such that if one O3 moves toward site I, the distance between the site I in the next six-ring window and the second O3 in that tetrahedron (labeled O3′ in the figure) cannot be similarly reduced without radical rearrangement of the framework. In other words, the coordination for Li^+ at site I can be optimized for only four out of the total of eight such

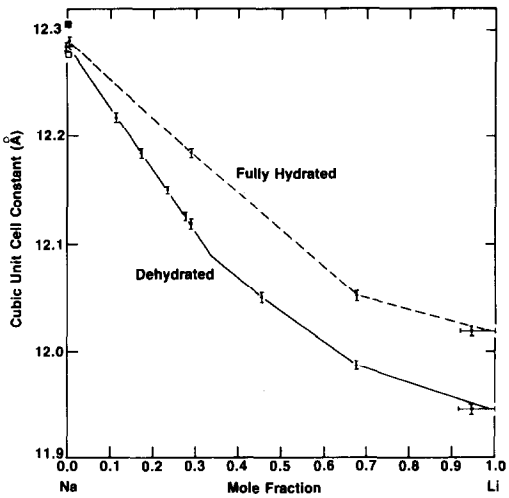

FIG. 4. The lattice constants of the cubic subcells of sodium/lithium zeolite A materials plotted against the extent of lithium exchange. For the pure sodium forms, the square symbols indicate the data of Pluth and Smith (□, Ref. (*2*)) and Gramlich and Meier (■, Ref. (*4*)). The vertical bars indicate the experimental uncertainties. The pure lithium form was prepared using multiple exchanges together with an intermediate calcination step. The indicated error in its composition reflects uncertainty associated with a presumed small quantity of a sodium-containing amorphous phase.

sites in any sodalite cage. These sites are arranged tetrahedrally as shown in Fig. 3. Interestingly, the rotation of one TO_4 is transmitted through the common O1 linkage to the facing four-ring window that completes the double four-ring unit. The sense of the rotation is *mirrored* through the plane defined by the four O1's.

At the present stage this argument remains qualitative, but it agrees with the conclusions reached from the NMR data (*10*). First, the plot of chemical shift against composition apparently indicates a linear decrease in the mean secant of the *T*–O–*T* angle with substitution up to the level $x = 0.33$, at which point there is a discontinuity. Beyond $x = 0.33$ the change is more gradual, indicating that the coordination requirements of the lithium are being accommodated differently. The variation of the lattice constant, a_0, with composition for the anhydrous materials is very similar in form. The reduction in a_0 is most marked during the initial stages of substitution and is linear with composition up to $x \approx 0.33$ (Fig. 4). For higher lithium concentrations the change is again more gradual and is no longer simply linear with composition. Second, the width of the ^{29}Si resonance is as narrow at $x = 0.33$ as at $x = 0$ (*10*), indicating that all ^{29}Si nuclei are equivalent at that composition. This equivalence is implicit to the model shown in Fig. 3.

This discussion has two structural implications for the Na_8Li_4–A ($x = 0.33$) material. First, from the chemical shift data we can use the correlation described above to predict a mean *T*–O–*T* angle of some 144°. Second, while the interpenetrating tetrahedra model still maintains cubic symmetry, there is no longer a center of symmetry at the center of the sodalite cage. The space group symmetry is lower than $Fm\bar{3}c$. Detailed structural results for this composition and for the fully exchanged lithium material will be of great interest.

Effect of Sorbed Water

Reflection intensity data from the $Na_{12}Li_0$–A and Na_8Li_4–A materials recorded at three different humidities are given in Table III. Hydration has a dramatic effect on the X-ray pattern, which is unremarkable as sorbed H_2O molecules contribute about 20% of the total number of electrons in the unit cell. The structure of the hydrated material is not known to a precision that is comparable with that of the anhydrous materials, and, indeed, the intensities calculated on the basis of the model described by Gramlich and Meier (*4*) do not agree particularly well with those observed from the present samples (Table III). Several calculated reflection intensity ratios do vary with cation substitution in a manner similar to that recorded for the anhydrous system. However, as there are substantial discrepancies between observed and calculated ratios for the sodium end-member, the same analysis could not be applied with confidence. Nonetheless the diffraction data do reveal certain features.

For the pure sodium form, the X-ray patterns recorded at ambient humidity and at a water vapor pressure of 20 mm Hg are quite similar (Table III). In contrast, for the Na_8Li_4–A material significant changes in the relative intensities accompany the same change in water vapor pressure. To determine whether these changes reflected much larger increases in water content than occur in the sodium form, the water loadings for the three samples Na_{12}–A, Na_8Li_4–A and Li_{12}–A were each monitored gravimetrically as a function of P_{H_2O}. The absorption isotherms for the three materials are similar in shape and they indicate that in each case about one additional water molecule per subcell is sorbed on changing the water vapor pressure from ambient to 20 mm Hg. The changes in the structure of the Na_8Li_4–A material between ambient and 20.6 mm

Hg cannot then be explained merely by gross changes in water content. We believe that they are associated with the exchange of cations between sites I and II/III invoked to account for the NMR data (*10*). This exchange is sensitive to the degree of hydration.

$$Li^{I} + Na^{II} \overset{H_2O}{\rightleftharpoons} Li^{II} + Na^{I}$$

A trend in the hydrated materials away from exclusive substitution of the site-I cations is generally consistent with the analysis of reflection intensity ratios mentioned above. The ^{29}Si chemical shift data from such materials (*10*) graphically illustrates that the change that occurs in the mean *T*–O–*T* angle is now smoothed over the whole composition field. The difference in lattice constants between the sodium and lithium end-members is also less marked in the hydrated materials (Fig. 4).

Conclusions

Where accurate structural data are available, comparison of observed and calculated powder reflection intensity ratios can be used to monitor changes in specific atomic parameters. In zeolites, this approach had previously been applied to monitoring changes in the distributions of cations of large atomic number. In the present study of anhydrous sodium/lithium zeolite A the usefulness of the technique has been extended to structures in which the contrast between the scattering from the framework and that from the cations is less marked. It is shown that the preferred site for lithium substitution is site I, in the six-ring face of the sodalite cages. As the lithium content increases, sodiums are continuously replaced in this site up to the composition Li_8Na_4–A.

A consideration of the possible modes of framework distortion that accompany lithium substitution indicates that of the eight six-ring sites in any sodalite cage the lithium coordination can be optimized for only four, arranged tetrahedrally.

Acknowledgments

We would like to thank J. Dunn for assistance with the X-ray measurements and a referee for several helpful comments on the manuscript.

References

1. D. W. Breck, W. G. Eversole, R. M. Milton, T. B. Reed, and T. L. Thomas, *J. Amer. Chem. Soc.* **78,** 5963 (1956).
2. J. J. Pluth and J. V. Smith, *J. Amer. Chem. Soc.* **102,** 4704 (1980).
3. W. J. Mortier, "Compilation of Extra Framework Sites in Zeolites," Butterworth, Surrey (1982).
4. V. Gramlich and W. M. Meier, *Z. Kristallogr.* **133,** 134 (1971).
5. CHEMGRAF Program Suite, E. K. Davies, Chemical Crystallography Laboratory, University of Oxford (1982).
6. R. M. Barrer, L. V. C. Rees, and D. J. Ward, *Proc. R. Soc. London Ser. A* **273,** 180 (1963).
7. Z. Dizdar, *J. Inorg. Nucl. Chem.* **34,** 1069 (1970).
8. P. Collin and R. Wey, *C.R. Acad. Sci. Paris Ser. D* **270,** 1069 (1970).
9. Z. Jirak, V. Bosacek, S. Vratislav, H. Herden, R. Schollner, W. J. Mortier, L. Gellens, and J. B. Uytterhoven, *Zeolites* **3,** 255 (1983).
10. M. T. Melchior, D. E. W. Vaughan, A. J. Jacobson, and C. F. Pictroski, *in* "Proceedings 6th International Zeolite Conference" D. H. Olson and A. Bisio, Eds. p. 684, Butterworth, Surrey (1984).
11. R. M. Milton, *U.S. Patent* 2,882,243 (1959).
12. H. M. Rietveld, *J. Appl. Crystallogr.* **2,** 65 (1969).
13. L. B. McCusker, *Zeolites* **4,** 51 (1984).
14. S. Gali, X. Solans, and M. Font Altaba, *J. Solid State Chem.* **46,** 172 (1983).
15. J. V. Smith, J. M. Bennett, and E. M. Flanigen, *Nature (London)* **215,** 241 (1967).
16. "International Tables for X-Ray Crystallography," Vol. IV, The Kynoch Press, Birmingham, England (1974).
17. J. V. Smith and C. S. Blackwell, *Nature (London)* **303,** 233 (1983).

18. R. H. JARMAN, *J. Chem. Soc. Chem. Commun.*, 512 (1983).
19. S. RAMDAS AND J. KLINOWSKI, *Nature (London)* **308,** 521 (1984).
20. A. M. GLAZER, *Acta Crystallogr. Sect. A* **31,** 756 (1975).
21. J. M. NEWSAM, in preparation.
22. O. JARCHOW, *Z. Kristallogr.* **122,** 407 (1965).
23. D. H. OLSON, *J. Phys. Chem.* **74,** 2758 (1970).
24. I. S. KERR, *Z. Kristallogr.* **139,** 186 (1974).
25. E. LIPPMAA, M. MAGI, A. SAMOSON, M. TARMAK, AND G. ENGELHARDT, *J. Amer. Chem. Soc.* **103,** 4992 (1981).
26. J. KLINOWSKI, J. M. THOMAS, C. A. FYFE AND J. S. HARTMAN, *J. Phys. Chem.* **85,** 2590 (1981).
27. D. E. W. VAUGHAN, M. T. MELCHIOR, AND A. J. JACOBSON, *ACS Symp. Ser.* **218,** 231 (1983).